

## Giant Helium Dimers Produced by Photoassociation of Ultracold Metastable Atoms

J. Léonard,\* M. Walhout,† A. P. Mosk,‡ T. Müller,§ M. Leduc, and C. Cohen-Tannoudji

*Ecole Normale Supérieure and Collège de France, Laboratoire Kastler Brossel, 24 rue Lhomond, 75231 Paris CEDEX 05, France*  
(Received 18 April 2003; revised manuscript received 19 June 2003; published 15 August 2003)

We produce giant, purely long-range helium dimers by photoassociation of metastable helium atoms in a magnetically trapped, ultracold cloud. The photoassociation laser is detuned close to the atomic  $2^3S_1 - 2^3P_0$  line and produces strong heating of the sample when resonant with molecular bound states. The temperature of the cloud serves as an indicator of the molecular spectrum. We report good agreement between our spectroscopic measurements and our calculations of the five bound states belonging to a  $0_u^+$  purely long-range potential well. These previously unobserved states have classical inner turning points of about  $150a_0$  and outer turning points as large as  $1150a_0$ .

DOI: 10.1103/PhysRevLett.91.073203

PACS numbers: 34.20.Cf, 32.80.Pj, 34.50.Gb

In the purely long-range molecules first proposed by Stwalley *et al.* [1], the binding potential, including the repulsive inner wall, depends only on the long-range part of the atom-atom interaction, and the internuclear distance is always large compared with ordinary chemical bond lengths. Theoretical description of these molecules involves the leading  $C_3/R^3$  terms of the electric dipole-dipole interaction and the fine structure inside each atom. These well-known interactions allow precise calculation of potential wells and rovibrational energies. Previous experimental studies of such spectra in alkali atoms have utilized the technique of laser-induced photoassociation (PA) in a magneto-optical trap (MOT) [2]. In addition to testing calculations of molecular structure, that work has produced precise measurements of excited-state lifetimes, and has led to accurate determinations of *s*-wave scattering lengths for alkali systems, which are of interest for studies of Bose-Einstein condensates (BECs) [3,4].

This Letter reports novel spectroscopic measurements and calculations for purely long-range molecules that are produced when two  $^4\text{He}$  atoms in the metastable  $2^3S_1$  ( $\text{He}^*$ ) state absorb laser light tuned close to the  $2^3S_1 - 2^3P_0$  ( $D_0$ ) atomic line at  $\lambda = 1083$  nm. The minimum internuclear distance in these dimers is unprecedentedly large, reaching values of  $150a_0$  ( $a_0 = 0.053$  nm), so retardation clearly influences the dipole-dipole interactions. Another unique feature is that each dimer is formed from two highly excited atoms carrying a total of 40 eV. Also, we have developed an original, “calorimetric” method for detecting the formation of these molecules. Instead of monitoring ion production rates, which are usually high for  $\text{He}^*$ , we measure the temperature increase of the cloud due to the presence of molecules. This turns out to be a great advantage, since Penning ionization, which would normally destabilize such energetic molecules, is strongly reduced as a consequence of the large internuclear distance in these giant dimers.

This is the first observation of purely long-range molecular states in  $\text{He}^*$ . Previous PA experiments were per-

formed in a  $\text{He}^*$  MOT [5], but with a PA laser tuned close to the  $2^3S_1 - 2^3P_2$  atomic line ( $D_2 \sim 32$  GHz below  $D_0$ ). There is no purely long-range potential linked to the  $2^3S_1 + 2^3P_2$  asymptote. The Utrecht group has also tried to observe the purely long-range states that we study here, near the  $D_0$  line, but without success [6]. We believe their lack of a result is explained by the fact that they monitor the ion production rate, which is strongly reduced for these states, as explained above.

Our experimental conditions differ significantly from the ones reported in [5]. The atoms are confined in a magnetic trap and cooled nearly to the BEC transition [7,8]. The phase space density is typically 6 orders of magnitude higher than in a MOT, so the PA process is much more efficient [9]. Also, the temperature is 2–3 orders of magnitude lower, so the Doppler broadening is small compared with the atomic natural line width  $\Gamma$ , which allows for improved spectroscopic precision. In addition, our magnetically trapped atoms are spin polarized in a single Zeeman sublevel of the  $2^3S_1$  state, so the initial quasimolecular state is  $^5\Sigma_g^+$ . Therefore, only *ungerade* excited states are accessible.

Figure 1 shows the only two potentials that can be excited in our experiment in the vicinity of the  $D_0$  atomic line. The photoassociation experiment consists in driving the transition from free pairs of  $2^3S_1$  atoms to bound states in the purely long-range  $0_u^+$  well connected to the  $2^3S_1 + 2^3P_0$  asymptote. Measurements of the bound-state spectrum proceed as follows. About  $10^9$  atoms are trapped in a MOT before being transferred into an Ioffe-Pritchard magnetostatic trap with a nonzero minimum  $B_0$  in the trapping magnetic field. An evaporative cooling sequence that utilizes RF-induced spin flips cools the atoms to 2–30  $\mu\text{K}$ . The critical temperature for Bose-Einstein condensation is in the range 1 to 4  $\mu\text{K}$ , depending on the density [7,11].

Figure 2 sketches the experimental setup and sequence for a typical PA experiment. After cooling, the cloud is illuminated for a few ms by light from a “PA laser” beam containing all polarization components relative to the magnetic-field axis. Just after this PA pulse, the cloud is

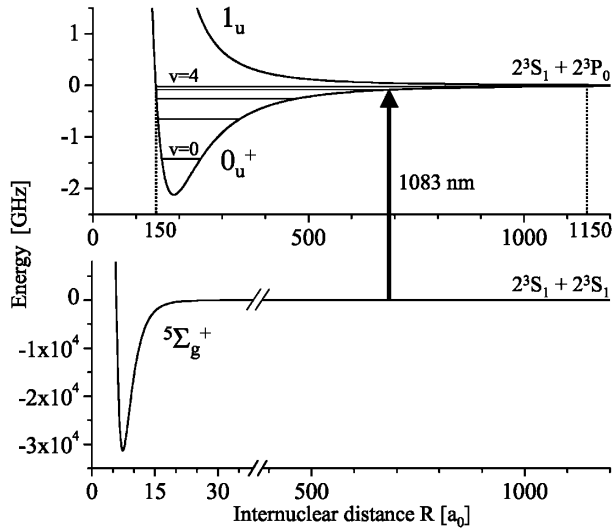


FIG. 1. Molecular potentials involved in the electronic excitation of two  $2^3S_1$  spin-polarized  $^4\text{He}$  atoms. The  $5^{\Sigma}_g^+$  potential is taken from [10]. Note the change in energy and length scales between the  $5^{\Sigma}_g^+$  and the purely long-range  $0_u^+$  potential wells. The excited potentials are calculated as described in the text and are the only experimentally accessible potentials linked to the  $2^3S_1 + 2^3P_0$  asymptote. Five bound states ( $v = 0$  to 4) are observed in the  $0_u^+$  well. Their inner turning points are around  $150a_0$ , their outer turning points range from  $250a_0$  ( $v = 0$ ) to  $1150a_0$  ( $v = 4$ ).

released and then detected by means of destructive absorption imaging after ballistic expansion. The number of atoms, the peak optical density, and the temperature are thereby measured as functions of the PA laser frequency.

Accurate spectroscopy is performed with a PA beam derived from a cavity-stabilized laser (width 0.3 MHz)

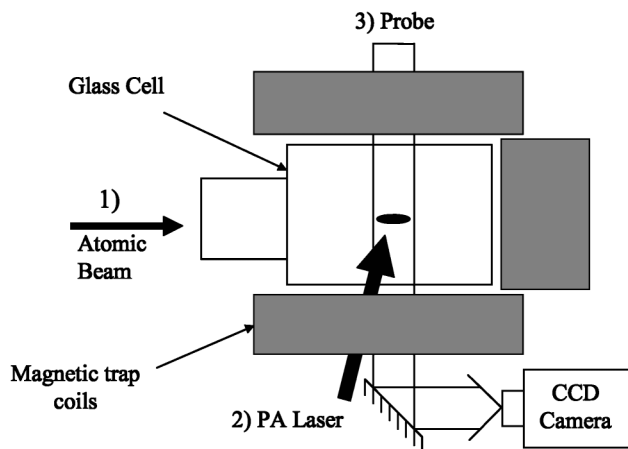


FIG. 2. Experimental setup. A detailed description has been published in [11]. (1) Metastable helium atoms are trapped and evaporated down to a few  $\mu\text{K}$  and a peak density of the order of  $10^{13} \text{ cm}^{-3}$ . (2) The cloud is illuminated inside the magnetic trap by the PA laser for a few ms. (3) The cloud is released. After ballistic expansion, it is imaged on a CCD camera with a magnification of 1.

073203-2

locked to the  $D_0$  line. The PA beam is tuned with sub-MHz precision to the molecular lines by acousto-optic modulators. With this technique, we can reach the four highest ( $v = 1$  to  $v = 4$ ) lines in the  $0_u^+$  well. For the  $v = 0$  line, the PA laser must be further detuned. In this case we use a temperature-tuned diode laser with a 3-MHz spectral width, as well as a Fabry-Perot cavity to measure its frequency relative to that of a reference laser locked to the  $D_2$  atomic line. The accuracy of the  $v = 0$  measurement is of the order of 10 MHz. The PA laser intensity is always set lower than or of the order of the atomic saturation intensity  $I_{\text{sat}} \sim 0.16 \text{ mW/cm}^2$ , and the exposure time between 0.1 and 10 ms. Figure 3 shows typical experimental data for the line  $v = 4$ . Figures 3(a) and 3(b) demonstrate that the peak optical density drops significantly when the PA beam is resonant with a molecular line, even if trap loss is weak. This situation is explained by the strong heating indicated in Fig. 3(c). The temperature increase provides a very sensitive diagnostic for resonances that produce little loss. Assuming that the heat deposited in the cloud is proportional to the number of molecules produced, we fit the frequency dependence of the temperature to a Lorentzian curve. The FWHM of the molecular lines is measured at low intensities to be 3.0(3) MHz, within the expected range for the molecular radiative width ( $\Gamma_{\text{mol}} \leq 2\Gamma$ ).

The heating mechanism that produces our signals can be roughly understood as follows. After absorbing a photon near the outer turning point, the molecular system can decay radiatively into two fast metastable atoms, each with a nonzero probability of being in the trapped state. Since the trap depth is 10 mK, fast atoms can remain trapped and heat up the cold cloud. This reasoning is supported by the fact that we can convert the heating

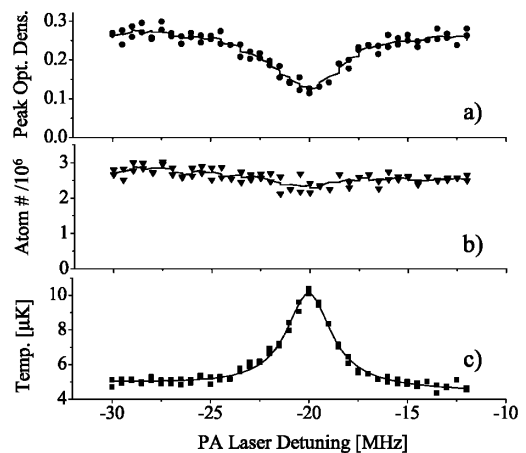


FIG. 3. Detection of the line  $v = 4$  in the  $0_u^+$  potential well. (a) Peak optical density, (b) atom number, and (c) temperature in  $\mu\text{K}$  versus PA laser frequency. Each point represents a new evaporated cloud after PA pulse illumination and ballistic expansion. The curves in graphs (a) and (b) indicate the averaging of data over five adjacent points. The curve in graph (c) is a Lorentzian fit to the data.

073203-2

into trap loss if, after the PA pulse, we apply an RF “knife” for 40 ms, thereby removing fast atoms from the trap. The simultaneous measurement of small trap loss and significant temperature increase suggests that each molecular excitation heats the sample considerably. This is the reason why the temperature probe is so sensitive.

Fits to our data give line centers  $\delta_\nu < 0$  for the molecular resonances, measured relative to the  $D_0$  atomic line. To obtain binding energies  $hb_\nu < 0$ , we must correct for shifts caused by the cloud’s finite temperature and the trap’s magnetic field. Since we are interested in a free-bound transition, the shifts arise from terms that explicitly represent the magnetic interaction and the relative motion of the initial  $2^3S_1$  pair. (The corresponding energies in the molecule are implicitly included in  $b_\nu$ .) The magnetic contribution can be written as  $2\mu B_0 + 3k_B T/2$ , where the second term exploits the equipartition theorem to express the average inhomogeneous Zeeman shift for a pair. The relative kinetic energy of the pair adds another shift of  $3k_B T/2$ . The derivation of this term in the  $s$ -wave limit, as well as consideration of line-broadening mechanisms, which we do not discuss here because we are mainly interested in the positions of the lines, will appear in a forthcoming paper. Finally, the binding energies are found to be  $hb_\nu = h\delta_\nu + 2\mu B_0 + 3k_B T$ . Additional recoil and mean-field shifts of the order of 10 kHz are negligible on the scale of our experimental uncertainties. We are not concerned with light shifts, since we use very low PA laser intensities; this is another advantage of the calorimetric technique over trap-loss measurements.

Each line is probed in different conditions of  $T$  (2–30  $\mu\text{K}$ ),  $B_0$  (300 mG–10 G), and density ( $10^{12}$ – $5 \times 10^{13}$   $\text{cm}^{-3}$ ). Within the accuracy of our experiment we find no density or magnetic-field dependence of the binding energies, and for each line we estimate an uncertainty of  $\pm 0.5$  MHz. Given this uncertainty and the range of magnetic field explored, we can infer an upper limit for the  $0_u^+$  magnetic moment of  $\sim 0.04$  Bohr magnetons [12].

In order to interpret the experimental frequency spectrum theoretically, we calculate the coupling between the atomic orbitals of one atom in the  $2^3S_1$  state and another in the  $2^3P_{J=0,1,2}$  state, which involves 54 molecular potentials. This coupling is constructed as a perturbative Hamiltonian in the basis of fine-structure-free atomic states. At large internuclear distances  $R$ , the lowest-order term of the electromagnetic interaction is the retarded dipole-dipole interaction [13,14], which is fully determined by the coefficient  $C_3 = (3/4)\hbar\Gamma/k^3$ , with  $\Gamma = 2\pi \times 1.6248$  MHz [15], and  $k = 2\pi/\lambda$ . This interaction includes no coupling between electronic orbital and spin angular momenta ( $\vec{L}$  and  $\vec{S}$ ) and is diagonal in the molecular Hund’s case (a) basis.

In the absence of  $\vec{L}$ - $\vec{S}$  coupling, the potential curves resulting from dipole-dipole interaction are purely attractive or repulsive and share a single asymptote. When we include the atomic fine structure in the Hamiltonian [16], the coupling gives rise to three distinct asymptotes and to

anticrossings between attractive and repulsive curves, leading to purely long-range potential wells [17]. We construct the fine-structure coupling phenomenologically from measured  $2^3P$  splittings [18,19]. If there is no rotation, the projection  $\Omega$  of the total electronic angular momentum on the molecular axis is a good quantum number. Our experiment probes the  $0_u^+$  purely long-range well plotted in Fig. 1.

We also consider how the rotation of the molecule can couple electronic states ( $\Delta\Omega = 0, \pm 1$ ), an effect that leaves  $\Omega = 0$  and  $0_u^+$  as only approximate labels. We add to the Hamiltonian the operator  $\hat{\ell}^2/(2\mu R^2)$  [20], where  $\hat{\ell} = \vec{J} - \vec{L} - \vec{S}$  is the angular momentum operator for the rotation of the molecule. As expected, the couplings with  $\Omega \neq 0$  become important when two potential curves determined in the nonrotating approximation cross each other. In the case of the  $0_u^+$  potential well, these crossings appear far enough in the classically forbidden region that we can neglect the nondiagonal rotation-induced couplings.

In the  $s$ -wave scattering regime, the initial ( $2^3S_1 + 2^3S_1$ ) pair exists only in the  $J = 2$  state. Elementary group theory and Bose-Einstein statistics for the nuclei [20] dictate that  $J$  in the excited state must be odd, namely, 1 or 3. Moreover, the Condon radius at which the transition occurs is so large that the excited molecule is in almost the same quantum state as a noninteracting pair of atoms in the  $2^3S_1 + 2^3P_0$  state [Hund’s case (c)]. Therefore  $J = 1$  is dominant.

The Hamiltonian including retarded dipole-dipole interaction, fine structure, and molecular rotation is diagonalized numerically. Adiabatic potentials are calculated with fixed internuclear distance, and an additional first order (diagonal) correction is applied to take into account the effect of the vibration of the nuclei on the electronic interaction energy. The  $0_u^+$  potential well depth calculated in this way for  $J = 1$  is 2.002 GHz. The five bound states measured in the well (see Fig. 1) have their inner turning points around  $150a_0$ . The outer turning point is as large as  $1150a_0$  for the  $\nu = 4$  vibrational state. From the discussion above, it is clear that even the repulsive, inner part of the potential has purely long-range character. The large internuclear distance is also the reason why the next-order term in  $C_6/R^6$  of the electromagnetic interaction is negligible [21]. More details about the theoretical approach will be given in a forthcoming paper [22].

Measured and calculated binding energies in the  $0_u^+$  well are presented in Table I. The measured spectrum agrees very well with the predicted  $J = 1$  progression from  $\nu = 1$  to  $\nu = 4$ . We also find good agreement for  $\nu = 0$ , though with less experimental accuracy. Although it is too weak to be observed, the  $J = 3$  progression has been calculated using the same model to illustrate the expected rotational splitting. Finally, comparison with calculated results for a nonretarded dipole-dipole interaction demonstrates the significant influence

TABLE I. Measured and calculated binding energies (in MHz) in the  $0_u^+$  well. The first column gives the experimental results. The two next columns give the results of the model described in the text for  $J = 1$  with and without including retardation effects. The last column contains calculated  $J = 3$  results with retardation.

	Experiment	Theory		
		$J = 1$	$J = 1^a$	$J = 3$
$\nu = 4$	-18.2 ( $\pm 0.5$ )	-18.12	-16.51	-3.791
$\nu = 3$	-79.6 ( $\pm 0.5$ )	-79.41	-76.79	-40.05
$\nu = 2$	-253.3 ( $\pm 0.5$ )	-252.9	-249.0	-172.3
$\nu = 1$	-648.5 ( $\pm 0.5$ )	-648.3	-643.1	-510.1
$\nu = 0$	-1430 ( $\pm 10$ )	-1418	-1411	-1209

<sup>a</sup>Calculated while neglecting retardation effects.

of retardation. We note that our measurement confirms the assumed value of  $C_3$  to within 0.2%.

In conclusion, we report the vibrational spectrum of a previously unobserved, purely long-range helium dimer produced in a very highly excited electronic state. Although the huge internal energy would allow it, the autoionization process is blocked by the extremely large size of the dimers. As an alternative to ion detection, we have developed a calorimetric detection scheme based on the heating of the atomic cloud by the radiative decay of the dimers. This technique merits further study. Finally, this Letter provides a foundation for a two-color, stimulated Raman experiment that would prepare molecules in the most weakly bound state of the  $^5\Sigma_g^+$  potential shown in Fig. 1, with the  $0_u^+$ ,  $\nu = 0$  state as an intermediate state. The corresponding Franck-Condon factor of  $\sim 0.1$  suggests that the transition rate should be high. The lifetime of these atypical dimers formed from two  $2^3S_1$  metastable atoms is unknown. Moreover, an accurate measurement of the  $s$ -wave elastic scattering length of  $2^3S_1$  helium should follow directly from the measured binding energy [3].

The authors thank Peter van der Straten (Utrecht), the Cold Atoms and Molecules group at Laboratoire Aimé Cotton, and the Cold Atoms group at Laboratoire Kastler Brossel for fruitful discussions. The work of A. P. M. is part of the research program of *Stichting voor Fundamenteel Onderzoek der Materie* (FOM) which is financially supported by *Nederlandse Organisatie voor Wetenschappelijk Onderzoek* (NWO). M.W. was partly funded by National Science Foundation Grant No. PHY-0140135, and T. M. by the *Procope* exchange program.

\*Electronic address: leonard@lkb.ens.fr

†Permanent address: Calvin College, Grand Rapids, MI, USA.

‡Permanent address: FOM Instituut voor Plasmafysica Rijnhuizen, and University of Twente, The Netherlands.

<sup>§</sup>Present address: Institut für Quantenoptik, Universität Hannover, Germany.

- [1] W. C. Stwalley, Y.-H. Uang, and G. Pichler, *Phys. Rev. Lett.* **41**, 1164 (1978).
- [2] See, e.g., review articles, W. C. Stwalley and H. Wang, *J. Mol. Spectrosc.* **195**, 194 (1999); J. Weiner, V. S. Bagnato, S. Zilio, and P. S. Julienne, *Rev. Mod. Phys.* **71**, 1 (1999); F. Masnou-Seeuws and P. Pillet, *Adv. At. Mol. Opt. Phys.* **47**, 53 (2001), and references therein.
- [3] E. R. I. Abraham, W. I. McAlexander, C. A. Sackett, and R. G. Hulet, *Phys. Rev. Lett.* **74**, 1315 (1995).
- [4] J. R. Gardner, R. A. Cline, J. D. Miller, D. J. Heinzen, H. M. J. M. Boesten, and B. J. Verhaar, *Phys. Rev. Lett.* **74**, 3764 (1995).
- [5] N. Herschbach, P. J. J. Tol, W. Vassen, W. Hogervorst, G. Woestenenk, J. W. Thomsen, P. van der Straten, and A. Niehaus, *Phys. Rev. Lett.* **84**, 1874 (2000).
- [6] P. van der Straten (private communication).
- [7] F. Pereira Dos Santos, J. Léonard, Junmin Wang, C. J. Barrelet, F. Perales, E. Rasel, C. S. Unnikrishnan, M. Leduc, and C. Cohen-Tannoudji, *Phys. Rev. Lett.* **86**, 3459 (2001).
- [8] A. Robert, O. Sirjean, A. Browaeys, J. Poupard, S. Nowak, D. Boiron, C. I. Westbrook, and A. Aspect, *Sci. Mag.* **292**, 463 (2001).
- [9] P. Pillet, A. Crubellier, A. Bleton, O. Dulieu, P. Nosbaum, I. Mourachko, and F. Masnou-Seeuws, *J. Phys. B* **30**, 2801 (1997).
- [10] J. Störck and W. Meyer, *Chem. Phys. Lett.* **225**, 229 (1991).
- [11] F. Pereira dos Santos, J. Leonard, Junmin Wang, C. J. Barrelet, F. Perales, E. Rasel, C. S. Unnikrishnan, M. Leduc, and C. Cohen-Tannoudji, *Eur. Phys. J. D* **19**, 103 (2002).
- [12] Since pure  $0_u^+$  states are not degenerate, only molecular rotation gives rise to a magnetic moment, which is therefore expected to be of the order of the nuclear magneton.
- [13] E. I. Dashevskaya, A. I. Voronin, and E. E. Nikitin, *Can. J. Phys.* **47**, 1237 (1969).
- [14] W. J. Meath, *J. Chem. Phys.* **48**, 227 (1968).
- [15] G. W. F. Drake, in *Atomic, Molecular and Optical Physics Handbook*, edited by G. W. F. Drake (AIP Press, New York, 1996), Chap. 11.
- [16] M. Movre and G. Pichler, *J. Phys. B* **10**, 2631 (1977).
- [17] The absence of hyperfine structure in  $^4\text{He}$  leads to relatively simple molecular potentials.
- [18] M. C. George, L. D. Lombardi, and E. A. Hessels, *Phys. Rev. Lett.* **87**, 173002 (2001), and references therein.
- [19] J. Castilleja, D. Livingston, A. Sanders, and D. Shiner, *Phys. Rev. Lett.* **84**, 4321 (2000), and references therein.
- [20] J. T. Hougen, *Natl. Bur. Stand. (U.S.)*, Monograph 115 (1970).
- [21] We estimate the  $C_6/R^6$  correction is at least 4 orders of magnitude smaller than  $C_3/R^3$  for an internuclear distance larger than  $150a_0$ .
- [22] The calculation exhibits two other ungerade purely long-range wells connected to the  $2^3S_1 + 2^3P_1$  asymptote. They are even shallower and support fewer bound states than the well examined here. Their inner turning points are over  $300a_0$ .